International Journal of Medical Microbiology 309 (2019) 151331

Contents lists available at ScienceDirect

International Journal of Medical Microbiology

journal homepage: www.elsevier.com/locate/ijmm

Investigating the assembly of the bacterial type III secretion system injectisome by *in vivo* photocrosslinking

Nidhi Singh[a], Samuel Wagner[a,b,*]

[a] University of Tübingen, Interfaculty Institute of Microbiology and Infection Medicine (IMIT), Elfriede-Aulhorn-Str. 6, 72076, Tübingen, Germany
[b] German Center for Infection Research (DZIF), partner-site Tübingen, Elfriede-Aulhorn-Str. 6, 72076 Tübingen Germany

ARTICLE INFO

Keywords:
Type III secretion
In vivo photocrosslinking
Macromolecular complexes
Complex assembly

ABSTRACT

Virulence-associated type III secretion systems serve the injection of bacterial effector proteins into eukaryotic host cells. These effector proteins modulate host cell biology in order to promote colonization and infection, hence type III secretion systems are often essential bacterial pathogenicity factors. The core of type III secretion systems is a cell envelope-spanning macromolecular machine called injectisome. It consists of almost twenty different components in a stoichiometry of one to more than one hundred. Assembly of this 6 MDa complex requires the coordinated integration of components from the cytoplasm, the inner membrane, the periplasm, the outer membrane and even the extracellular space of Gram-negative bacteria. Here, we review injectisome assembly with an emphasis on the techniques that were employed towards its investigation. In particular, we focus on *in vivo* photocrosslinking, a technique that exploits the encoding of the artificial UV-inducible crosslinking amino acid *p*-benzoyl-phenylalanine to identify protein-protein interactions and to delineate assembly pathways.

1. Introduction

The export of proteins is instrumental for the interaction of bacteria with their environment. Bacteria export proteins of diverse functions, like toxins, adhesion factors, effector proteins, transcription factors, or proteases. Protein export across the cell envelope of Gram-positive bacteria is relatively simple as only one membrane needs to be passed. Export occurs mostly by means of the Sec and Tat translocons that translocate unfolded and folded substrate proteins across the cytoplasmic membrane, respectively (Hamed et al., 2018). Protein export across the two membranes of the cell envelope of Gram-negative bacteria requires more elaborate mechanisms. To date, nine different protein secretion systems, termed type I to type IX, have been identified that differ in the buildup of their machines, energization of secretion (ATP vs. PMF, or both), secretion signal, and folding state of their substrates (unfolded vs. folded), and whether they secrete proteins in one step or in two steps across the two membranes of the cell envelope (Costa et al., 2015). Three of these secretion systems (type III, type IV, and type VI) even serve the introduction of bacterial proteins directly into the cytosol of target cells (Fig. 1A) (Galán and Waksman, 2018). These injection machines constitute large protein complexes of usually more than 100 subunits, several megadalton in size. Often, they consist of cytosolic, inner membrane, periplasmic, outer membrane, and extracellular components. Assembly of these machines is an intricate and costly task that requires precise orchestration and is often highly regulated at multiple levels. In this review, we focus on the current state of our understanding of the assembly of the type III secretion injectisome (Fig. 1B), whose secretion system is also found in bacterial flagella. We will particularly emphasize the methodology that has been used towards elucidating assembly mechanisms. More elaborate reviews of assembly, structure and function of T3SS can be found elsewhere (Deng et al., 2017; Diepold and Wagner, 2014; Galán et al., 2014; Wagner et al., 2018). We will refer to the unified nomenclature of type III secretion systems (T3SS) throughout (Fig. 1C) (Hueck, 1998; Portaliou et al., 2016).

2. Structure and function of the injectisome

2.1. Base

The injectisome base is composed of 12–15 subunits of the outer membrane secretin SctC and 24 subunits each of the inner membrane proteins SctD and SctJ (Fig. 1B) (Schraidt and Marlovits, 2011; Worrall et al., 2016). SctC forms a closed gate in the outer membrane that is opened upon assembly of the needle filament (Hu et al., 2018; Worrall et al., 2016). SctD and SctJ build two concentric rings in the periplasm

* Corresponding author at: University of Tübingen, Interfaculty Institute of Microbiology and Infection Medicine (IMIT), Elfriede-Aulhorn-Str. 6, 72076, Tübingen, Germany.
E-mail address: samuel.wagner@med.uni-tuebingen.de (S. Wagner).

https://doi.org/10.1016/j.ijmm.2019.151331
Received 19 February 2019; Received in revised form 9 July 2019; Accepted 12 July 2019

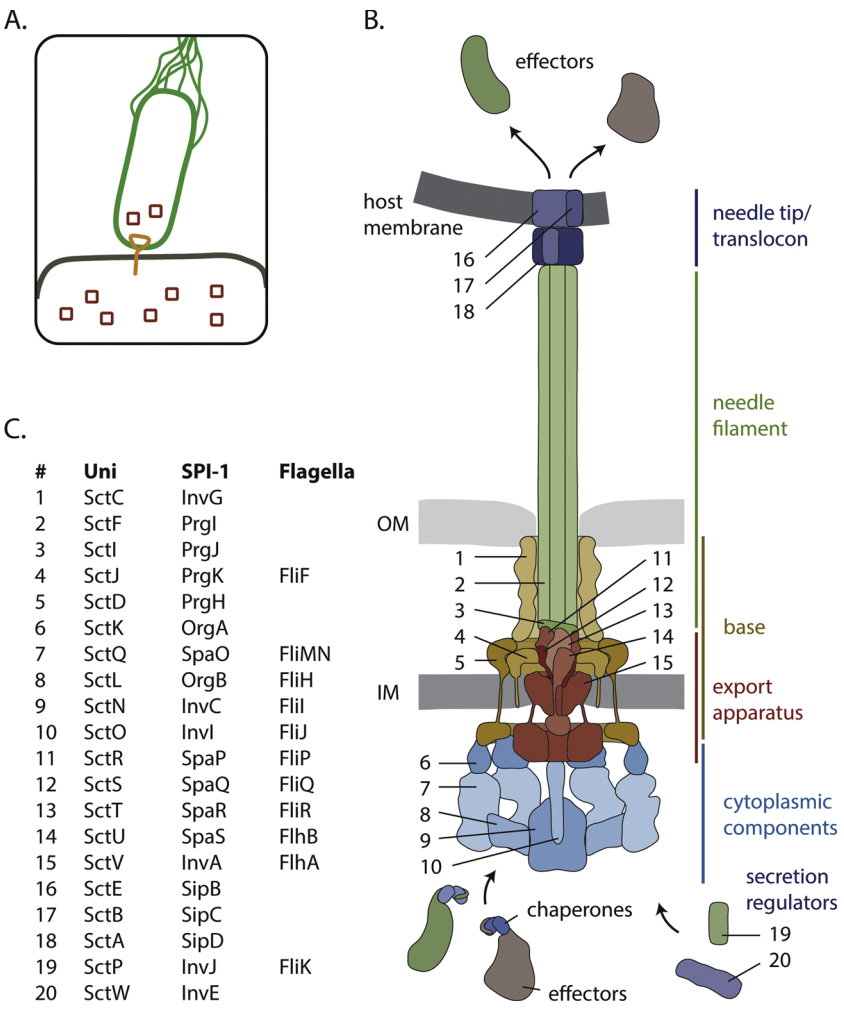

C.

#	Uni	SPI-1	Flagella
1	SctC	InvG	
2	SctF	PrgI	
3	SctI	PrgJ	
4	SctJ	PrgK	FliF
5	SctD	PrgH	
6	SctK	OrgA	
7	SctQ	SpaO	FliMN
8	SctL	OrgB	FliH
9	SctN	InvC	FliI
10	SctO	InvI	FliJ
11	SctR	SpaP	FliP
12	SctS	SpaQ	FliQ
13	SctT	SpaR	FliR
14	SctU	SpaS	FlhB
15	SctV	InvA	FlhA
16	SctE	SipB	
17	SctB	SipC	
18	SctA	SipD	
19	SctP	InvJ	FliK
20	SctW	InvE	

Fig. 1. Cartoon of the assembly of the T3SS injectisome. Protein names are indicated by their last letter, omitting "Sct". The assembly pathways are drawn from left to right. A. Assembly of the inner membrane export apparatus starts with membrane-integrated SctR. SctR (and also SctS and SctT, not shown) folds into a conformation that permits helical assembly. Then, five SctR, followed by one SctT and four SctS assemble into a helical assembly, winding up from the membrane. Recruitment of one SctU and then nine SctV finish export apparatus assembly, which is then enhoused by 24 subunits of the inner ring protein SctJ. B. 15 secretin subunits assemble, supported by pilotins, into a pre-pore. The secretin forms a pore in the outer membrane and recruits the outer inner ring protein SctD. Closure of the outer inner ring is not permitted until the SctJ-export apparatus assembly has been incorporated. Recruitment of the cytoplasmic components and subsequent assembly of the needle filament complete assembly of the injectisome. Abbreviations: IM, inner membrane; OM, outer membrane; PG, peptidoglycan. This figure is adapted with permission from reference (Wagner et al., 2018).

with SctJ forming the inner and SctD forming the outer ring. While SctJ comprises an N-terminal lipid anchor and often a C-terminal transmembrane segment (TMS), SctD has a small N-terminal domain in the cytoplasm followed by a single TMS and a sizable periplasmic domain that interacts with SctJ and with the N-terminus of SctC (Schraidt et al., 2010). Traditionally, base and the below-introduced export apparatus and needle filament have been referred to as needle complex.

2.2. Cytoplasmic components

SctK, SctQ, SctL, SctN, and SctO are the cytoplasmic components of the injectisome (Fig. 1B). SctK, SctQ, and SctL constitute the so-called sorting platform that has been implicated in binding chaperone-substrate complexes according to the hierarchy state of secretion (Lara-Tejero et al., 2011). SctK and SctQ form six pods that bind through a single SctK to the cytoplasmic domains of four SctD, each (Hu et al., 2017, 2015). Due to an internal start codon, *sctQ* is translated into two polypeptides of different lengths ($SctQ_{FL}$ and $SctQ_{C}$) and the presence of both polypeptides is essential for injectisome assembly and T3SS function (Bzymek et al., 2012; Diepold et al., 2015; Lara-Tejero et al., 2019; McDowell et al., 2016; Song et al., 2017; Yu et al., 2011), however, $SctQ_{C}$ may not be a structural component of the pods (Lara-Tejero et al., 2019). Stoichiometry estimates based on fluorescence microscopy (Diepold et al., 2017; Zhang et al., 2017) and structural analysis of SctQ complexes (Bzymek et al., 2012; McDowell et al., 2016; Notti et al., 2015) suggest that 24 $SctQ_{FL}$ are associated with each injectisome, 4 $SctQ_{FL}$ per pod. A homodimer of SctL connects each of the six pods to the hexameric ATPase SctN (Diepold et al., 2017; Hu et al., 2017; Imada et al., 2016; Notti et al., 2015) that is believed to support stripping of chaperones and substrate unfolding (Akeda and Galán, 2005; Erhardt et al., 2014). A single SctO is located at the center of the SctN hexamer and protrudes towards the cytoplasmic domain of the major export apparatus protein SctV (B. Hu et al., 2017; Ibuki et al., 2011; Majewski et al., 2019). SctK, SctQ, SctL, and SctN were also found as soluble complexes in the cytoplasm (Diepold et al., 2017, 2015; Johnson and Blocker, 2008; Zhang et al., 2017). Dynamic exchange of soluble and injectisome-associated complexes may be relevant for T3SS substrate targeting and secretion.

2.3. Export apparatus

The export apparatus of T3SS consists of five hydrophobic proteins that are highly conserved in injectisome and flagellar T3SS: SctR, SctS, SctT, SctU, and SctV (Fig. 1B) (Wagner et al., 2010). Five SctR, four SctS, one SctT, and one SctU form a unique helical assembly within the SctJ ring of the base, on the periplasmic side of the inner membrane (Dietsche et al., 2016; Johnson et al., 2019; Kuhlen et al., 2018, 2019; Zilkenat et al., 2016). They seem to gate the export channel and form the basis for assembly of the needle filament. In addition to contributing its predicted TMS to this helical assembly, SctU contains a cytoplasmic C-terminal domain that undergoes autocleavage at a conserved NPTH motif (Allaoui et al., 1994; Deane et al., 2008; Lountos et al., 2009; Wiesand et al., 2009; Zarivach et al., 2008). Autocleavage of SctU is critical for switching of secretion from early to intermediate substrates, hence SctU is also called switch protein (Ferris et al., 2005; Lavander et al., 2002; Minamino and Macnab, 2000; Monjarás Feria

et al., 2015). It was proposed to mediate injection of substrates into the secretion channel formed by SctV, SctRSTU, and the filament proteins (Evans et al., 2013). Also SctV is located within the central inner membrane patch of the base (Fig. 1B) (Abrusci et al., 2012). The N-terminal half of SctV forms a transmembrane domain (TMD) with 8 predicted TMS. Its C-terminal half is exposed to the cytoplasm, forming a nonameric ring with a central pore of 50 Å in diameter (Abrusci et al., 2012). $SctV_C$ is involved in establishing the substrate secretion hierarchy by binding secretion adapter proteins for early and intermediate substrates (e.g., the gatekeeper SctW) (Diepold et al., 2012; Gaytán et al., 2018; Portaliou et al., 2017; Yu et al., 2018) as well as substrate-chaperone complexes (Bange et al., 2010; Portaliou et al., 2017; Xing et al., 2018). The N-terminal TMDs of SctV serve to utilize the inner membrane proton motive force for secretion (Erhardt et al., 2017; Hara et al., 2011; Minamino et al., 2011) and possibly form the actual substrate translocation channel in the inner membrane (Fig. 1B).

2.4. Filament, needle tip and translocon

The helical needle filament is composed of more than 100 copies of SctF (Broz et al., 2007). It is connected to the distal end of the SctRSTU complex by about six copies of the inner rod protein SctI (Fig. 1B) (Dietsche et al., 2016; Kuhlen et al., 2018; Marlovits et al., 2006; Torres-Vargas et al., 2019; Zilkenat et al., 2016). The inner lumen of the needle shapes a right handed spiral, surfaced with polar and hydrophobic residues. Its axial diameter is 15 Å, which only allows passage of unfolded substrates (Hu et al., 2018; Loquet et al., 2012). The needle of most injectisomes ends with a pentameric needle tip complex formed by the hydrophilic translocator protein SctA (Broz et al., 2007; Epler et al., 2012; Mueller et al., 2005). Penetration of the host cell membrane is achieved by formation of a so-called translocon complex, which is composed of multiple copies of two different hydrophobic translocator proteins, SctB and SctE (Dickenson et al., 2013; Montagner et al., 2011; Park et al., 2018). These proteins are predicted to contain 1–2 TMS that insert into host cell membranes with support from the tip complex (Marenne et al., 2003). Translocon assembly within these membranes may be influenced by host factors like Rac1 (Nauth et al., 2018).

3. Assembly of the injectisome

Assembly of the injectisome is a highly coordinated process to ensure the efficient formation of secretion- and membrane translocation-competent machines. Two phases of injectisome assembly are distinguished: assembly of the principle secretion-competent machine – relying on Sec-mediated translocation and membrane insertion of many of its components – and type III secretion-dependent assembly of the needle filament, tip, and translocon. Here, we will only consider the type III secretion-independent assembly. We will discuss injectisome – and if relevant, flagellar – assembly according to the methodology that was used for its investigation.

3.1. Electron microscopy

Early electron micrographs of isolated flagellar basal bodies of wild type *Salmonella* Typhimurium and a wide array of flagellar gene deletion mutants indicated that flagellar assembly starts with formation of the membrane and supramembrane (MS) ring in the inner membrane (Kubori et al., 1992). The MS ring, which is composed of FliF (Fig. 1C), was the minimal observable unit, whose formation did not require the presence of any other structural component. An analogous genetic and electron microscopic analysis of the assembly of the *Salmonella* injectisome showed that base structures could form in the absence of all non-base components (Sukhan et al., 2001). When *Salmonella* inner ring proteins SctD and SctJ were overexpressed in *Escherichia coli*, ring structures were observed by electron microscopy (Kimbrough and Miller, 2000). All these data indicated that assembly of flagella and injectisomes starts with formation of the inner ring (or MS ring) structures of the base, and that this ring formation is independent of other T3SS components. Consequently, an assembly model was proposed in which the inner membrane export apparatus components were recruited after inner ring formation (Sukhan et al., 2001). This model was no longer plausible when it became clear that the export apparatus components were housed within the membrane patch of the inner rings of the base (Fig. 1B) (Wagner et al., 2010): the two-dimensional nature of the membrane does not permit integration of the export apparatus after completion of the inner rings.

Why did these early studies come to the wrong conclusions, though? These studies focused on observing ring structures by electron microscopy. Clearly, these ring structures could assemble in the absence of export apparatus components. What was not assessed, however, was the efficiency of assembly of these structures; no quantification of assembly was performed or reported. And so it was eventually missed that efficiency of assembly of the inner rings was strongly compromised in the absence of the export apparatus components. Similarly, it was concluded that the genetic organization of injectisome components does not play a role in assembly as assembled needle complexes could be observed by cryo-electron microscopy upon total gene scrambling and rewiring of post-transcriptional regulation. However, it was found that the yield of isolated needle complexes dropped by more than 80%, indicating severe problems in assembly efficiency as a consequence of these genetic perturbations (Song et al., 2017).

3.2. Blue native PAGE

In order to allow for a qualitative and quantitative assessment of needle complex assembly, including base and export apparatus components, we developed mild, non-ionic detergent-based purification protocols and blue native PAGE analysis of these large complexes (Wagner et al., 2010; Zilkenat et al., 2016, 2017). Blue native PAGE is an electrophoretic method to investigate the composition of membrane protein complexes (Schägger and von Jagow, 1991). It relies on the mild extraction of membrane proteins and membrane protein complexes by nonionic detergents that are expected to preserve the native protein conformation. Charging and electrophoretic migration of the extracted proteins is facilitated by the adsorption of the anionic, water-soluble blue dye Coomassie G to the hydrophobic regions of the extracted membrane proteins, which are then separated based on their complex size in gradient gels of a Tricine-based PAGE (Wittig et al., 2006).

Using blue native PAGE we could show that all export apparatus components intimately associate with the needle complex base and that the core components SctR and SctT are housed at the center of the base (Wagner et al., 2010). We could further show that base assembly is nucleated by prior assembly of SctR, SctS, and SctT, and that also recruitment of SctU and SctV depends on these small export apparatus components (Fig. 2). In agreement with previous work, also our study showed that base assembly is possible in the absence of export apparatus components but our data made clear that assembly efficiency drops by 80–90% in the absence of SctRST. Using blue native PAGE we could further show that assembly of a complex of the flagellar SctR and SctT homologs FliP and FliR is chaperoned by FliO, a small bitopic membrane protein whose gene almost always preceeds the gene of FliP in flagella (Fabiani et al., 2017). Why FliO is so critical for FliPR assembly while the close homologs SctRT do apparently not require an assembly chaperone is not known at this point (Fabiani et al., 2017; Fukumura et al., 2017).

Blue native PAGE analysis of sucrose gradient-fractionated *Salmonella* showed that the cytoplasmic injectisome component SctQ forms a large complex whose formation is independent of any base or export apparatus component, or of the ATPase SctN, but to a substantial degree dependent on the other cytoplasmic components SctK and SctL (Lara-Tejero et al., 2011). In fact, SctK and SctL were shown to associate

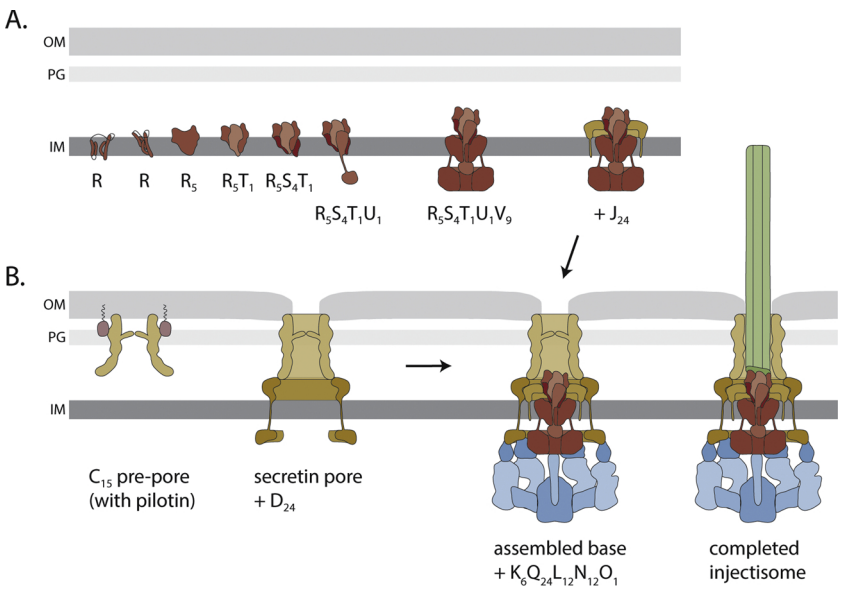

Fig. 2. Cartoon of the assembly of the T3SS injectisome. Protein names are indicated by their last letter, omitting "Sct". The assembly pathways are drawn from left to right. **A.** Assembly of the inner membrane export apparatus starts with membrane-integrated SctR. SctR (and also SctS and SctT, not shown) folds into a conformation that permits helical assembly. Then, five SctR, followed by one SctT and four SctS assemble into a helical assembly, winding up from the membrane. Recruitment of one SctU and then nine SctV finish export apparatus assembly, which is then enhoused by 24 subunits of the inner ring protein SctJ. **B.** 15 secretin subunits assemble, supported by pilotins (purple), into a pre-pore. The secretin forms a pore in the outer membrane and recruits the outer inner ring protein SctD. Closure of the outer inner ring is not permitted until the SctJ-export apparatus assembly has been incorporated. Recruitment of the cytoplasmic components and subsequent assembly of the needle filament complete assembly of the injectisome. Abbreviations: IM, inner membrane; OM, outer membrane; PG, peptidoglycan. This figure is adapted with permission from reference (Wagner et al., 2018) (For interpretation of the references to colour in this figure legend, the reader is referred to the web version of this article.).

with SctQ and this tripartite complex bound T3SS chaperone-substrate complexes according to the hierarchy state of secretion.

While the development of mild detergent-based blue native PAGE protocols provided a much better access to the analysis of injectisome assembly, the approach was limited to complexes and subcomplexes that were sufficiently stable and abundant to be detected, which is not the case for every assembly intermediate. In the case of the injectisome this was limited to a highly stable SctRT complex, the secretin complex in the outer membrane, the base, and the sorting platform.

3.3. Fluorescence microscopy

Fluorescence microscopy is highly complementary to biochemical techniques to elucidate the assembly of protein complexes. Following the localization of fluorophore-labelled proteins of interest relative to each other allows for the *in vivo* analysis of assembly without the need for protein extraction or complex purification. The approach is particularly powerful when state-of-the-art super-resolution microscopy is applied to assess assembly kinetics and co-localization of individual complex components. Unfortunately, it is very challenging, if not impossible, to obtain functionally tagged variants of proteins in the core of complexes without exposed termini, small proteins, or very hydrophobic proteins, so only assembly of a subset of complex components can be addressed by this approach. Furthermore, only indirect information on protein-protein interaction can be obtained. Fluorescence microscopy is also limited in distinguishing assembled and non-assembled states of a protein of interest, unless distinct localizations can be observed (Zoued and Diepold, 2017). This limitation can be overcome by the complementary diffusion analysis using fluorescence correlation spectroscopy (Diepold et al., 2017). Despite of these limitations, our insight of assembly of type III secretion injectisomes has benefited much from analysis by fluorescence microscopy. Early studies showed in *Yersinia* that assembly of the secretin ring occurred independently of other injectisome components (Diepold et al., 2010). They also showed that the outer inner ring protein SctD assembled at the secretin, rather than assembling together with the inner inner ring protein SctJ around the export apparatus components (Fig. 2B) (Diepold et al., 2010). It was further shown that the core cytoplasmic component SctQ as well as the ATPase SctN form specific foci at the membrane, whose formation depended on the presence of all other cytoplasmic components, the base components, and to some degree even on the export apparatus components (Diepold et al., 2010), a finding that was later corroborated for a T3SS of *Salmonella* (Zhang et al., 2017).

The only export apparatus component whose assembly was analyzed by fluorescence microcopy to date is SctV. It was shown to assemble into SctC-co-localizing immobile foci in wild type bacteria but not in mutants lacking the core export apparatus components SctR, SctS, and SctT (Diepold et al., 2011). SctV foci also assembled in mutants lacking the base components, but these foci were mobile in the membrane. These data supported our notion that the export apparatus assembles independently, starting with SctRST. The assembling export apparatus is unrestricted in the inner membrane, until it is housed in by the base, immobilizing the complex by penetration of the peptidoglycan layer (Fig. 2B). Fluorescence microscopic analysis of the flagellar SctV homolog FlhA yielded somewhat conflicting results. While it was shown in one study that formation of the inner membrane MS ring is promoted by prior assembly of the SctV homolog FlhA (Li and Sourjik, 2011), FlhA expression had no effect on MS ring assembly in a later study (Morimoto et al., 2014). However, as shown for injectisomes, formation of FlhA foci depended on the presence of the SctR, SctS, and SctT homologs FliP, FliQ, and FliR, respectively (Morimoto et al., 2014).

3.4. In vivo photocrosslinking

To overcome the limitations of both, blue native PAGE analysis and fluorescence microscopy, in assessing assembly of the hydrophobic export apparatus components and in capturing assembly intermediates we extensively employed *in vivo* photocrosslinking.

In vivo photocrosslinking is based on the genetic encoding and translational incorporation of the artificial amino acid *p*-benzoyl-phenylalanine (*p*Bpa) at a position of choice of a protein of interest (Fig. 3A) (Farrell et al., 2005). The encoding is established by an amber stop codon that is suppressed by a *p*Bpa-charged suppressor tRNA. Charging of the tRNA is accomplished by a mutated tRNA synthetase from *Methanococcus jannaschii* (Chin et al., 2002). *p*Bpa crosslinks to the peptide backbone of nearby proteins in response to UV irradiation at 365 nm. Suppression of amber stop codons is well tolerated by bacteria like *Escherichia coli* or *Salmonella* Typhimurium that contain only few natural amber stop codons (about 5%). The efficiency of suppression of the amber stop codon is influenced by the stop codon's genetic context (Miller and Albertini, 1983); in our hands it varied between 50% and close to 100% (Dietsche et al., 2016). Since the incorporation of the crosslinking amino acid *p*Bpa occurs during translation, even inaccessible positions like within the membrane or those buried in the core of proteins or protein complexes can be approached (Fig. 3C-D).

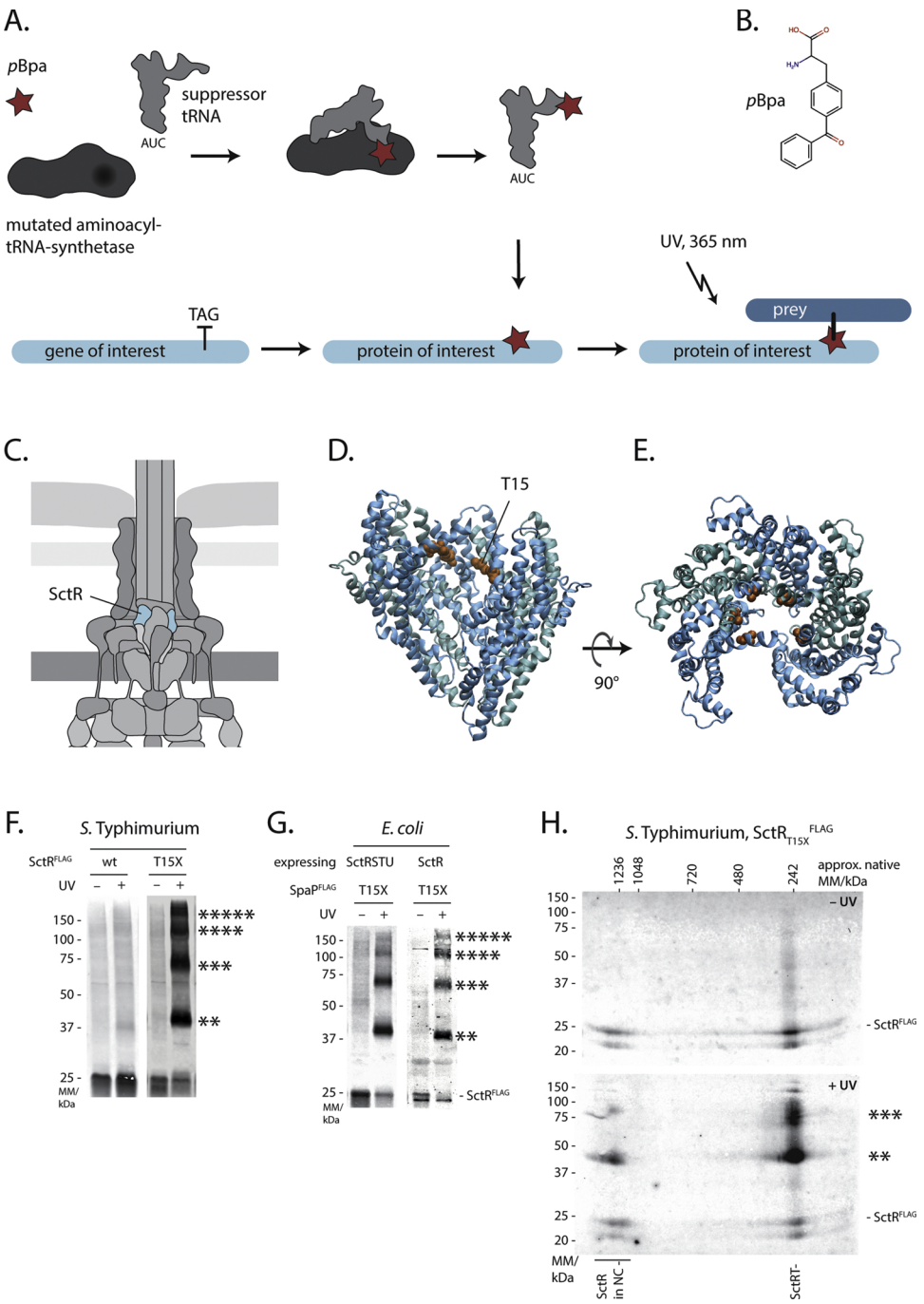

Fig. 3. *In vivo* photocrosslinking. A. Concept of encoding pBpa. An amber stop codon-recognizing suppressor tRNA is charged with pBpa by a mutated aminoacyl-tRNA synthetase. A gene of interest containing an amber stop codon at a desired position gets translated into a protein of interest containing pBpa. Upon UV irradiation, pBpa crosslinks to nearby proteins. B. Structure of pBpa. C. – H. Crosslinking example from Salmonella pathogenicity island-1 encoded SctR (Dietsche et al., 2016). C. Position of SctR in the assembled injectisome. D. & E. Structure of the flagellar SctR homolog FliP of S. Typhimurium (PDB 6F2D, (Kuhlen et al., 2018)) indicating Tyr-52, which corresponds to Tyr-15 in SctR. In the experiments shown in F-H, Tyr-15 was replaced by pBpa. F. Immunodetection of chromosome-encoded SctRFLAG or SctRT15XFLAG on Western blots of crude membrane samples of S. Typhimurium separated by SDS PAGE. Each sample is shown with and without UV-irradiation to induce photocrosslinking of pBpa to neighboring interaction partners. Asterisks indicate the different multimers of SctR (2-5). G. Immunodetection of SctRFLAG on Western blots of crude membrane samples of E. coli BL21 (DE3) expressing SctRT15XFLAG together with SctSTU or in the absence of all other T3SS components. The results show that SctR assembly occurs independent of any other T3SS component. H. Immunodetection of SctRT15XFLAG on Western blots of crude membrane samples of S. Typhimurium separated by 2-dimensional blue native/SDS PAGE. SctR crosslinks up to a SctR trimer can be detected in the SctRT complex as well as in the assembled needle complex.

While being a strength, encoding the crosslinker is also one of the techniques major limitation as a single mutant needs to be made and tested for every position of interest. Primary identification of protein-protein crosslinks can easily be achieved by SDS PAGE, Western blotting, and immunodetection of the bait protein: UV-irradiation-dependent bands of the bait above the monomeric form indicate productive crosslinks to prey (Fig. 3F). Identification of the prey can be achieved by reciprocal immunodetection, or by enrichment or purification followed by mass spectrometry.

The following rationale helps choosing suitable positions for *p*Bpa incorporation to identify protein-protein interactions: If a structure of the protein complex is known, *p*Bpa is placed at or near the protein-protein interaction site, preferably replacing amino acid residues of similar size and properties as *p*Bpa (Phe, Trp, Tyr) or those that are little conserved. Guidance can be obtained from the software tool SNAP[2] that predicts functional effects of sequence variants of each amino acid position of a given protein (Hecht et al., 2015). If the site of interaction between two proteins is not known, prediction of protein-protein interaction based on covariance analysis is a powerful tool facilitating identification of interacting residues (Hopf et al., 2014). This approach was very successfully used to map the interaction of the switch protein SctU and the minor export apparatus proteins SctRST (Kuhlen et al., 2019). The predictive power of covariance analysis strongly depends on the number of homologs of the interacting proteins. If too few homologs are known, scanning of the known (from structure) or predicted surface of the protein of interest by replacing various exposed residues with *p*Bpa may yield identification of interaction partners and interaction sites. Transmembrane proteins offer an additional clue through prediction of their transmembrane topology by software tools like TOPCONS (Tsirigos et al., 2015): Firstly, residues at the relevant side of the

membrane can be chosen. Secondly, each alpha helical TMS can be scanned for interactors by probing towards each side of the helix.

The observation of a *p*Bpa crosslink tells that a given assembly step has occurred. We call them signature crosslinks for a given protein-protein interaction. One or several signature crosslinks between each pair of interacting proteins thus easily allows to track assembly without the necessity to purify the complex or to solve the structure of the interacting proteins. Analyzing the occurrence of signature crosslinks in the wild type and relevant mutants allows to draw conclusions on the conditions that need to be met to allow assembly of this particular protein complex (Fig. 3G).

We set out to identify protein-protein interactions of the export apparatus components SctR and SctS by probing amino acid positions within each predicted TMS (Dietsche et al., 2016). Several crosslinks could be identified, specifying interactions between different SctR (up to five), SctR and SctS, SctR and SctT, SctR and SctU. By analyzing these crosslinks in different mutant backgrounds we could conclude that assembly starts with formation of five SctR, proceeds through recruitment of SctS and SctT, to recruitment of SctU (Fig. 2). Interaction of SctS and SctT depended on the presence of SctR but not on SctU. Also the helical structure of the complex of the flagellar SctRSTU homologs FliPQR/FlhB suggests that assembly starts with five SctR and proceeds through subsequent recruitment of one SctT, four SctS, and one SctU (Kuhlen et al., 2019). This notion is further supported by the observation that a stable complex of FliP and FliR also forms in the absence of FliQ (Fabiani et al., 2017). Completion of this core export apparatus SctRSTU complex occurred independent of the major export apparatus protein SctV or the inner ring protein SctJ, as judged by formation of a SctR-SctU crosslink.

We further scanned the inner surface of the inner ring protein SctJ by *p*Bpa crosslinking to map the interaction between the base and the export apparatus (Kuhlen et al., 2018). We identified interactions between SctJ and SctR as well as between SctJ and SctT. Initially, these results left us puzzled since the identified SctJ residues were located far above the inner membrane and the core export apparatus was assumed to be mostly within the membrane plane. Solution of the structure of the assembled flagellar FliPQR complex by cryo-electron microscopy and docking of this complex into cryo-electron microscopic and cryo-electron tomographic structures of the injectisome base, however, substantiated a supramembrane position of this complex. How the SctRSTU complex rises out of the membrane and is fixed in its final supramembrane position remains to be investigated. Rising of the complex out of the membrane may occur through the stepwise recruitment of subunits. The energy released by the strongly hydrophobic protein-protein interactions of the assembling subunits may suffice for extraction of the growing complex from the membrane. Formation of the SctV ring around the assembled SctRSTU complex may further drive the lifting of the helical SctRSTU complex from the membrane and support interaction with SctJ and formation of the 24-mer SctJ ring. SctV, however, is only necessary for needle complex assembly in some T3SS (Diepold et al., 2010) while it is completely dispensable in others (Dietsche et al., 2016; Wagner et al., 2010).

Particularly useful for the analysis of complex assembly proved to be the visualization of *in vivo* photocrosslinks by 2-dimensional blue native/SDS PAGE (Zilkenat et al., 2017). While the observation of a crosslink by SDS PAGE reveals the existence of an interaction, it does not tell whether the interaction occurs in an assembly intermediate, in the final complex, or even in a dead end aggregate. By resolving the protein complexes in a native dimension before subjecting them to denaturing SDS PAGE, we were able to distinguish these different possibilities and show, e.g., that an observed SctR-SctR interaction involving Tyr-15 occurred in an SctRT assembly intermediate and in the injectisome (Fig. 3H) (Dietsche et al., 2016).

Incorporation of *p*Bpa at different positions of a protein of interest does not only aid in the identification of protein-protein interactions but at the same time *p*Bpa mutants serve in assessing the functional relevance of the mutated amino acid residues. *p*Bpa is a rather bulky aromatic residue that may interfere with intra- as well as intermolecular packing and thus affect protein folding, complex assembly or function. Of the 144 different *p*Bpa mutants that we reported to date, 51 showed a defect in type III secretion (Dietsche et al., 2016; Krampen et al., 2018; Kuhlen et al., 2019, 2018; Torres-Vargas et al., 2019). Interestingly, many of these secretion-deficient mutants yielded productive crosslinks, indicating that specific functional mechanisms rather than protein folding or complex assembly were compromised in these mutants. Overall, *p*Bpa seems to be accommodated rather well despite of its bulky nature.

3.5. Cryo-electron tomography

More recently, cryo-electron tomography has allowed to address structure and composition of large protein complexes *in situ* (Oikonomou and Jensen, 2016). By analyzing the structure of deletion mutants of different complex components, information on complex assembly can be gained. Cryo-electron tomographic analysis of assembly of the T3SS injectisome showed that formation of the cytoplasmic pods strictly required the presence of SctK, SctQ, and SctL, while the ATPase SctN was less critical in a *Salmonella* T3SS (Hu et al., 2017). The stalk protein SctO was entirely dispensable for pod formation and for recruitment of the ATPase SctN. Contrary to the observations made by fluorescence microscopy, assembly of the cytoplasmic pods was not affected by deletion of export apparatus components, neither by deletion of SctV, nor of SctRSTU. However, since a quantification of co-observation events of bases and pods was missing, hard conclusions on the requirements of assembly cannot be drawn. Intriguingly, it could be shown that the cytoplasmic N-terminal domain of the inner ring protein SctD remodeled from an even 24-mer to six clusters of four domains upon assembly of the pods. In addition, the analysis structurally corroborated the observation made previously by blue native PAGE analysis and fluorescence microscopy, namely that SctV is not required for SctRST assembly but that SctV requires SctRSTU for recruitment to the base.

4. Conclusions

The use of different complementary biochemical and microscopic techniques has revealed the principle order of assembly of the bacterial type III secretion system injectisome. Assembly of the cell envelope-embedded needle complex is initiated at two sites independently, with the outer membrane secretin on the one hand, and with the core inner membrane export apparatus at the other hand (Fig. 2). We proposed that dependence of base assembly on nucleation by the export apparatus ensures secretion competence while dependence of base assembly on secretin formation ensures outer membrane translocation, thus, needle complex assembly comprises an inherent quality control mechanism (Diepold and Wagner, 2014). Assembly of the cytoplasmic apparatus seems to rely almost equally much oπn all its components except the stalk protein.

In vivo photocrosslinking has allowed us to gain insight into the steps of assembly of the core export apparatus components, proteins that had been shown to be largely inaccessible by other techniques. In particular, the covariance analysis-guided selection of *p*Bpa positions and the analysis of crosslinks by two-dimensional blue native/SDS PAGE turned out to be very powerful for the identification and characterization of protein-protein interactions. In the future, the exact mapping of the crosslinking sites by mass spectrometry will enable an even deeper investigation of the mechanisms of assembly.

A major drawback in most studies of injectisome assembly has been the delineation of assembly steps from the analysis of deletion mutants. Deletion of structural components may perturb the assembly pathway, so that one risks an over-interpretation of the relevance of the observed assembly product. To gain a better understanding of assembly without

the shortcomings of deletion mutants, we will need to study the kinetics of assembly at a molecular level. This may be achieved by synchronizing assembly and a by combination of pulse-chase labelling with *in vivo* photocrosslinking to follow the occurrence of crosslinks over the time of assembly.

Acknowledgements

Work in the laboratory of Samuel Wagner related to this article was supported by the Deutsche Forschungsgemeinschaft (DFG) as part of the Collaborative Research Center (SFB) 766 Bacterial Cell Envelope, project B14.

References

Abrusci, P., Vergara-Irigaray, M., Johnson, S., Beeby, M.D., Hendrixson, D.R., Roversi, P., Friede, M.E., Deane, J.E., Jensen, G.J., Tang, C.M., Lea, S.M., 2012. Architecture of the major component of the type III secretion system export apparatus. Nat. Struct. Mol. Biol. 20, 99–104.

Akeda, Y., Galán, J.E., 2005. Chaperone release and unfolding of substrates in type III secretion. Nature 437, 911–915.

Allaoui, A., Woestyn, S., Sluiters, C., Cornelis, G.R., 1994. YscU, a *Yersinia enterocolitica* inner membrane protein involved in Yop secretion. J. Bacteriol. 176, 4534–4542.

Bange, G., Kümmerer, N., Engel, C., Bozkurt, G., Wild, K., Sinning, I., 2010. FlhA provides the adaptor for coordinated delivery of late flagella building blocks to the type III secretion system. Proc. Natl. Acad. Sci. U. S. A. 107, 11295–11300.

Broz, P., Mueller, C.A., Müller, S.A., Philippsen, A., Sorg, I., Engel, A., Cornelis, G.R., 2007. Function and molecular architecture of the *Yersinia* injectisome tip complex. Mol. Microbiol. 65, 1311–1320.

Bzymek, K.P., Hamaoka, B.Y., Ghosh, P., 2012. Two translation products of *Yersinia* yscQ assemble to form a complex essential to type III secretion. Biochemistry 51, 1669–1677.

Chin, J.W., Martin, A.B., King, D.S., Wang, L., Schultz, P.G., 2002. Addition of a photocrosslinking amino acid to the genetic code of Escherichiacoli. Proc. Natl. Acad. Sci. U. S. A. 99, 11020–11024.

Costa, T.R.D., Felisberto-Rodrigues, C., Meir, A., Prevost, M.S., Redzej, A., Trokter, M., Waksman, G., 2015. Secretion systems in Gram-negative bacteria: structural and mechanistic insights. Nat. Rev. Microbiol. 13, 343–359.

Deane, J.E., Graham, S.C., Mitchell, E.P., Flot, D., Johnson, S., Lea, S.M., 2008. Crystal structure of Spa40, the specificity switch for the *Shigella flexneri* type III secretion system. Mol. Microbiol. 69, 267–276.

Deng, W., Marshall, N.C., Rowland, J.L., McCoy, J.M., Worrall, L.J., Santos, A.S., Strynadka, N.C.J., Finlay, B.B., 2017. Assembly, structure, function and regulation of type III secretion systems. Nat. Rev. Microbiol. 15, 323–337. https://doi.org/10.1038/nrmicro.2017.20.

Dickenson, N.E., Choudhari, S.P., Adam, P.R., Kramer, R.M., Joshi, S.B., Middaugh, C.R., Picking, W.L., Picking, W.D., 2013. Oligomeric states of the *Shigella* translocator protein IpaB provide structural insights into formation of the type III secretion translocon. Protein Sci. 22, 614–627.

Diepold, A., Amstutz, M., Abel, S., Sorg, I., Jenal, U., Cornelis, G.R., 2010. Deciphering the assembly of the *Yersinia* type III secretion injectisome. EMBO J. 29, 1928–1940.

Diepold, A., Kudryashev, M., Delalez, N.J., Berry, R.M., Armitage, J.P., 2015. Composition, formation, and regulation of the cytosolic C-ring, a dynamic component of the type III secretion injectisome. PLoS Biol. 13, e1002039.

Diepold, A., Sezgin, E., Huseyin, M., Mortimer, T., Eggeling, C., Armitage, J.P., 2017. A dynamic and adaptive network of cytosolic interactions governs protein export by the T3SS injectisome. Nat. Commun. 8, 1–12.

Diepold, A., Wagner, S., 2014. Assembly of the bacterial type III secretion machinery. FEMS Microbiol. Rev. 38, 802–822.

Diepold, A., Wiesand, U., Amstutz, M., Cornelis, G.R., 2012. Assembly of the *Yersinia* injectisome: the missing pieces. Mol. Microbiol. 85, 878–892.

Diepold, A., Wiesand, U., Cornelis, G.R., 2011. The assembly of the export apparatus (YscR,S,T,U,V) of the *Yersinia* type III secretion apparatus occurs independently of other structural components and involves the formation of an YscV oligomer. Mol. Microbiol. 82, 502–514.

Dietsche, T., Tesfazgi Mebrhatu, M., Brunner, M.J., Abrusci, P., Yan, J., Franz-Wachtel, M., Schärfe, C., Zilkenat, S., Grin, I., Galán, J.E., Kohlbacher, O., Lea, S., Macek, B., Marlovits, T.C., Robinson, C.V., Wagner, S., 2016. Structural and functional characterization of the bacterial type III secretion export apparatus. PLoS Pathog. 12, e1006071.

Epler, C.R., Dickenson, N.E., Bullitt, E., Picking, W.L., 2012. Ultrastructural analysis of IpaD at the tip of the nascent MxiH type III secretion apparatus of Shigella flexneri. J. Mol. Biol. 420, 29–39.

Erhardt, M., Mertens, M.E., Fabiani, F.D., Hughes, K.T., 2014. ATPase-independent type-III protein secretion in Salmonella enterica. PLoS Genet. 10, e1004800.

Erhardt, M., Wheatley, P., Kim, E.A., Hirano, T., Zhang, Y., Sarkar, M.K., Hughes, K.T., Blair, D.F., 2017. Mechanism of type-III protein secretion: regulation of FlhA conformation by a functionally critical charged-residue cluster. Mol. Microbiol. 104, 234–249.

Evans, L.D.B., Poulter, S., Terentjev, E.M., Hughes, C., Fraser, G.M., 2013. A chain mechanism for flagellum growth. Nature 504, 287–290.

Fabiani, F.D., Renault, T.T., Peters, B., Dietsche, T., Gálvez, E.J.C., Guse, A., Freier, K., Charpentier, E., Strowig, T., Franz-Wachtel, M., Macek, B., Wagner, S., Hensel, M., Erhardt, M., 2017. A flagellum-specific chaperone facilitates assembly of the core type III export apparatus of the bacterial flagellum. PLoS Biol. 15, e2002267–24.

Farrell, I.S., Toroney, R., Hazen, J.L., Mehl, R.A., Chin, J.W., 2005. Photo-cross-linking interacting proteins with a genetically encoded benzophenone. Nat. Methods 2, 377–384.

Ferris, H.U., Furukawa, Y., Minamino, T., Kroetz, M.B., Kihara, M., Namba, K., Macnab, R.M., 2005. FlhB regulates ordered export of flagellar components via autocleavage mechanism. J. Biol. Chem. 280, 41236–41242.

Fukumura, T., Makino, F., Dietsche, T., Kinoshita, M., Kato, T., Wagner, S., Namba, K., Imada, K., Minamino, T., 2017. Assembly and stoichiometry of the core structure of the bacterial flagellar type III export gate complex. PLoS Biol. 15, e2002281–22.

Galán, J.E., Lara-Tejero, M., Marlovits, T.C., Wagner, S., 2014. Bacterial type III secretion systems: specialized nanomachines for protein delivery into target cells. Annu. Rev. Microbiol. 68, 415–438.

Galán, J.E., Waksman, G., 2018. Protein-injection machines in bacteria. Cell 172, 1306–1318.

Gaytán, M.O., Monjarás Feria, J., Soto, E., Espinosa, N., Benítez, J.M., Georgellis, D., González-Pedrajo, B., 2018. Novel insights into the mechanism of SepL-mediated control of effector secretion in enteropathogenic *Escherichia coli*. MicrobiologyOpen 7, e00571.

Hamed, M.B., Anné, J., Karamanou, S., Economou, A., 2018. Streptomyces protein secretion and its application in biotechnology. FEMS Microbiol. Lett. 365.

Hara, N., Namba, K., Minamino, T., 2011. Genetic characterization of conserved charged residues in the bacterial flagellar type III export protein FlhA. PLoS One 6, e22417.

Hecht, M., Bromberg, Y., Rost, B., 2015. Better prediction of functional effects for sequence variants. BMC Genomics 16 (Suppl 8), S1.

Hopf, T.A., Schärfe, C.P.I., Rodrigues, J.P.G.L.M., Green, A.G., Kohlbacher, O., Sander, C., Bonvin, A.M.J.J., Marks, D.S., 2014. Sequence co-evolution gives 3D contacts and structures of protein complexes. Elife 3, 65.

Hu, B., Lara-Tejero, M., Kong, Q., Galán, J.E., Liu, J., 2017. In situ molecular architecture of the *Salmonella* type III secretion machine. Cell 168 1065–1074.e10.

Hu, B., Morado, D.R., Margolin, W., Rohde, J.R., Arizmendi, O., Picking, W.L., Picking, W.D., Liu, J., 2015. Visualization of the type III secretion sorting platform of Shigella flexneri. Proc. Natl. Acad. Sci. U. S. A. 112, 1047–1052.

Hu, J., Worrall, L.J., Hong, C., Vuckovic, M., Atkinson, C.E., Caveney, N., Yu, Z., Strynadka, N.C.J., 2018. Cryo-EM analysis of the T3S injectisome reveals the structure of the needle and open secretin. Nat. Commun. 9, 3840.

Hueck, C.J., 1998. Type III protein secretion systems in bacterial pathogens of animals and plants. Microbiol. Mol. Biol. Rev. 62, 379–433.

Ibuki, T., Imada, K., Minamino, T., Kato, T., Miyata, T., Namba, K., 2011. Common architecture of the flagellar type III protein export apparatus and F- and V-type ATPases. Nat. Struct. Mol. Biol.

Imada, K., Minamino, T., Uchida, Y., Kinoshita, M., Namba, K., 2016. Insight into the flagella type III export revealed by the complex structure of the type III ATPase and its regulator. Proc. Natl. Acad. Sci. U. S. A. 113, 3633–3638.

Johnson, S., Blocker, A., 2008. Characterization of soluble complexes of the Shigella flexneri type III secretion system ATPase. FEMS Microbiol. Lett. 286, 274–278.

Johnson, S., Kuhlen, L., Deme, J.C., Abrusci, P., Lea, S.M., 2019. The structure of an injectisome export gate demonstrates conservation of architecture in the core export gate between flagellar and virulence type III secretion systems. MBio 10, 111.

Kimbrough, T.G., Miller, S.I., 2000. Contribution of *Salmonella typhimurium* type III secretion components to needle complex formation. Proc. Natl. Acad. Sci. U. S. A. 97, 11008–11013.

Krampen, L., Malmsheimer, S., Grin, I., Trunk, T., Lührmann, A., De Gier, J.-W., Wagner, S., 2018. Revealing the mechanisms of membrane protein export by virulence-associated bacterial secretion systems. Nat. Commun. 9, 3467.

Kubori, T., Shimamoto, N., Yamaguchi, S., Namba, K., Aizawa, S., 1992. Morphological pathway of flagellar assembly in Salmonella typhimurium. J. Mol. Biol. 226, 433–446.

Kuhlen, L., Abrusci, P., Johnson, S., Gault, J., Deme, J., Caesar, J., Dietsche, T., Mebrhatu, M.T., Ganief, T., Macek, B., Wagner, S., Robinson, C.V., Lea, S.M., 2018. Structure of the core of the type III secretion system export apparatus. Nat. Struct. Mol. Biol. 25, 583–590.

Kuhlen, L., Johnson, S., Zeitler, A., Bäurle, S., Deme, J.C., Debo, R., Fisher, J., Wagner, S., Lea, S.M., 2019. The flagellar substrate specificity switch protein FlhB assembles onto the extra-membrane export gate to regulate type three secretion. bioRxiv 20 https://doi.org/10.1101/686782. 99–20.

Lara-Tejero, M., Kato, J., Wagner, S., Liu, X., Galán, J.E., 2011. A sorting platform determines the order of protein secretion in bacterial type III systems. Science 331, 1188–1191.

Lara-Tejero, M., Qin, Z., Hu, B., Butan, C., Liu, J., Galán, J.E., 2019. Role of SpaO in the assembly of the sorting platform of a *Salmonella* type III secretion system. PLoS Pathog. 15, e1007565.

Lavander, M., Sundberg, L., Edqvist, P.J., Lloyd, S.A., Wolf-Watz, H., Forsberg, A., 2002. Proteolytic cleavage of the FlhB homologue YscU of *Yersinia pseudotuberculosis* is essential for bacterial survival but not for type III secretion. J. Bacteriol. 184, 4500–4509.

Li, H., Sourjik, V., 2011. Assembly and stability of flagellar motor in Escherichia coli. Mol. Microbiol.

Loquet, A., Sgourakis, N.G., Gupta, R., Giller, K., Riedel, D., Goosmann, C., Griesinger, C., Kolbe, M., Baker, D., Becker, S., Lange, A., 2012. Atomic model of the type III secretion system needle. Nature 486, 276–279.

Lountos, G.T., Austin, B.P., Nallamsetty, S., Waugh, D.S., 2009. Atomic resolution structure of the cytoplasmic domain of *Yersinia pestis* YscU, a regulatory switch

involved in type III secretion. Protein Sci. 18, 467–474.
Majewski, D.D., Worrall, L.J., Hong, C., Atkinson, C.E., Vuckovic, M., Watanabe, N., Yu, Z., Strynadka, N.C.J., 2019. Cryo-EM structure of the homohexameric T3SS ATPase-central stalk complex reveals rotary ATPase-like asymmetry. Nat. Commun. 10, 1–12.
Marenne, M.-N., Journet, L., Mota, L.J., Cornelis, G.R., 2003. Genetic analysis of the formation of the Ysc-Yop translocation pore in macrophages by *Yersinia enterocolitica*: role of LcrV, YscF and YopN. Microb. Pathog. 35, 243–258.
Marlovits, T.C., Kubori, T., Unger, V.M., Galán, J.E., 2006. Assembly of the inner rod determines needle length in the type III secretion injectisome. Nature 441, 637–640.
McDowell, M.A., Marcoux, J., McVicker, G., Johnson, S., Fong, Y.H., Stevens, R., Bowman, L.A., Bowman, L.A.H., Degiacomi, M.T., Yan, J., Wise, A., Friede, M.E., Friede, M., Benesch, J.L.P., Deane, J.E., Tang, C.M., Robinson, C.V., Lea, S.M., 2016. Characterisation of *Shigella* Spa33 and *Thermotoga* FliM/N reveals a new model for C-ring assembly in T3SS. Mol. Microbiol. 99, 749–766.
Miller, J.H., Albertini, A.M., 1983. Effects of surrounding sequence on the suppression of nonsense codons. J. Mol. Biol. 164, 59–71.
Minamino, T., Macnab, R.M., 2000. Domain structure of *Salmonella* FlhB, a flagellar export component responsible for substrate specificity switching. J. Bacteriol. 182, 4906–4914.
Minamino, T., Morimoto, Y.V., Hara, N., Namba, K., 2011. An energy transduction mechanism used in bacterial flagellar type III protein export. Nat. Commun. 2, 475.
Monjarás Feria, J.V., Lefebre, M.D., Stierhof, Y.-D., Galán, J.E., Wagner, S., 2015. Role of autocleavage in the function of a type III secretion specificity switch protein in *Salmonella enterica* serovar Typhimurium. MBio 6, e01459–15.
Montagner, C., Arquint, C., Cornelis, G.R., 2011. Translocators YopB and YopD from *Yersinia* form a multimeric integral membrane complex in eukaryotic cell membranes. J. Bacteriol. 193, 6923–6928.
Morimoto, Y.V., Ito, M., Hiraoka, K.D., Che, Y.-S., Bai, F., Kami-Ike, N., Namba, K., Minamino, T., 2014. Assembly and stoichiometry of FliF and FlhA in *Salmonella* flagellar basal body. Mol. Microbiol. 91, 1214–1226.
Mueller, C.A., Broz, P., Müller, S.A., Ringler, P., Erne-Brand, F., Sorg, I., Kuhn, M., Engel, A., Cornelis, G.R., 2005. The V-antigen of *Yersinia* forms a distinct structure at the tip of injectisome needles. Science 310, 674–676.
Nauth, T., Huschka, F., Schweizer, M., Bosse, J.B., Diepold, A., Failla, A.V., Steffen, A., Stradal, T.E.B., Wolters, M., Aepfelbacher, M., 2018. Visualization of translocons in Yersinia type III protein secretion machines during host cell infection. PLoS Pathog. 14, e1007527.
Notti, R.Q., Bhattacharya, S., Lilic, M., Stebbins, C.E., 2015. A common assembly module in injectisome and flagellar type III secretion sorting platforms. Nat. Commun. 6, 7125.
Oikonomou, C.M., Jensen, G.J., 2016. A new view into prokaryotic cell biology from electron cryotomography. Nat Rev Micro 14, 205–220.
Park, D., Lara-Tejero, M., Waxham, M.N., Li, W., Hu, B., Galán, J.E., Liu, J., 2018. Visualization of the type III secretion mediated *Salmonella*-host cell interface using cryo-electron tomography. Elife 7, e39514.
Portaliou, A.G., Tsolis, K.C., Loos, M.S., Balabanidou, V., Rayo, J., Tsirigotaki, A., Crepin, V.F., Frankel, G., Kalodimos, C.G., Karamanou, S., Economou, A., 2017. Hierarchical protein targeting and secretion is controlled by an affinity switch in the type III secretion system of enteropathogenic Escherichia coli. EMBO J. 36 e201797515–3531.
Portaliou, A.G., Tsolis, K.C., Loos, M.S., Zorzini, V., Economou, A., 2016. Type III secretion: building and operating a remarkable nanomachine. Trends Biochem. Sci. 41, 175–189.
Schägger, H., von Jagow, G., 1991. Blue native electrophoresis for isolation of membrane protein complexes in enzymatically active form. Anal. Biochem. 199, 223–231.
Schraidt, O., Lefebre, M.D., Brunner, M.J., Schmied, W.H., Schmidt, A., Radics, J., Mechtler, K., Galán, J.E., Marlovits, T.C., 2010. Topology and organization of the *Salmonella typhimurium* type III secretion needle complex components. PLoS Pathog. 6, e1000824.
Schraidt, O., Marlovits, T.C., 2011. Three-dimensional model of *Salmonella*'s needle complex at subnanometer resolution. Science 331, 1192–1195.
Song, M., Sukovich, D.J., Ciccarelli, L., Mayr, J., Fernandez-Rodriguez, J., Mirsky, E.A., Tucker, A.C., Gordon, D.B., Marlovits, T.C., Voigt, C.A., 2017. Control of type III protein secretion using a minimal genetic system. Nat. Commun. 8, 14737.
Sukhan, A., Sukhan, A., Kubori, T., Kubori, T., Wilson, J., Wilson, J., Galán, J.E., Galán, J.E., 2001. Genetic analysis of assembly of the *Salmonella enterica* serovar Typhimurium type III secretion-associated needle complex. J. Bacteriol. 183, 1159–1167.
Torres-Vargas, C.E., Kronenberger, T., Roos, N., Dietsche, T., Poso, A., Wagner, S., 2019. The inner rod of virulence-associated type III secretion systems constitutes a needle adapter of one helical turn that is deeply integrated into the system's export apparatus. Mol. Microbiol. https://doi.org/10.1111/mmi.14327.
Tsirigos, K.D., Peters, C., Shu, N., Käll, L., Elofsson, A., 2015. The TOPCONS web server for consensus prediction of membrane protein topology and signal peptides. Nucleic Acids Res. 43, W401–7.
Wagner, S., Grin, I., Malmsheimer, S., Singh, N., Torres-Vargas, C.E., Westerhausen, S., 2018. Bacterial type III secretion systems: a complex device for the delivery of bacterial effector proteins into eukaryotic host cells. FEMS Microbiol. Lett. 365, e1002983.
Wagner, S., Königsmaier, L., Lara-Tejero, M., Lefebre, M., Marlovits, T.C., Galán, J.E., 2010. Organization and coordinated assembly of the type III secretion export apparatus. Proc. Natl. Acad. Sci. U. S. A. 107, 17745–17750.
Wiesand, U., Sorg, I., Amstutz, M., Wagner, S., van den Heuvel, J., Lührs, T., Cornelis, G.R., Heinz, D.W., 2009. Structure of the type III secretion recognition protein YscU from *Yersinia enterocolitica*. J. Mol. Biol. 385, 854–866. https://doi.org/10.1016/j.jmb.2008.10.034.
Wittig, I., Braun, H.-P., Schägger, H., 2006. Blue native PAGE. Nat. Protoc. 1, 418–428.
Worrall, L.J., Hong, C., Vuckovic, M., Deng, W., Bergeron, J.R.C., Majewski, D.D., Huang, R.K., Spreter, T., Finlay, B.B., Yu, Z., Strynadka, N.C.J., 2016. Near-atomic-resolution cryo-EM analysis of the *Salmonella* T3S injectisome basal body. Nature 540, 597–601.
Xing, Q., Shi, K., Portaliou, A., Rossi, P., Economou, A., Kalodimos, C.G., 2018. Structures of chaperone-substrate complexes docked onto the export gate in a type III secretion system. Nat. Commun. 9, 1773.
Yu, X.-J., Grabe, G.J., Liu, M., Mota, L.J., Holden, D.W., 2018. SsaV interacts with SsaL to control the translocon-to-effector switch in the *Salmonella* SPI-2 type three secretion system. MBio 9, 379.
Yu, X.-J., Liu, M., Matthews, S., Holden, D.W., 2011. Tandem translation generates a chaperone for the *Salmonella* type III secretion system protein SsaQ. J. Biol. Chem. 286, 36098–36107.
Zarivach, R., Deng, W., Vuckovic, M., Felise, H.B., Nguyen, H.V., Miller, S.I., Finlay, B.B., Strynadka, N.C.J., 2008. Structural analysis of the essential self-cleaving type III secretion proteins EscU and SpaS. Nature 453, 124–127.
Zhang, Y., Lara-Tejero, M., Bewersdorf, J., Galán, J.E., 2017. Visualization and characterization of individual type III protein secretion machines in live bacteria. Proc. Natl. Acad. Sci. U. S. A. 114, 6098–6103.
Zilkenat, S., Dietsche, T., Monjarás Feria, J.V., Torres-Vargas, C.E., Mebrhatu, M.T., Wagner, S., 2017. Blue native PAGE analysis of bacterial secretion complexes. Methods Mol. Biol. 1615, 321–351.
Zilkenat, S., Franz-Wachtel, M., Stierhof, Y.-D., Galán, J.E., Macek, B., Wagner, S., 2016. Determination of the stoichiometry of the complete bacterial type III secretion needle complex using a combined quantitative proteomic approach. Mol. Cell Proteomics 15, 1598–1609.
Zoued, A., Diepold, A., 2017. Defining assembly pathways by fluorescence microscopy. Methods Mol. Biol. 1615, 289–298.